Plasticity and an Inverse Brittle-to-Ductile Transition in Strontium Titanate

P. Gumbsch, S. Taeri-Baghbadrani, D. Brunner, W. Sigle, and M. Rühle
Max-Planck-Institut für Metallforschung,
Seestraße 92, 70174 Stuttgart, Germany

(Received 10 April 2001; published 6 August 2001)

The use of ceramic materials is often restricted by a transition from ductile behavior to brittle fracture with decreasing temperature. For example, strontium titanate ($SrTiO_3$) is known to be extremely fragile and brittle below 1300 K. It is therefore surprising to find that $SrTiO_3$ single crystals can be deformed in compression below 1050 K again. Extensive plastic deformation up to 7% strain at low yield stresses of the order of only 120 MPa is possible at room temperature. Low temperature plasticity is carried by the same $\langle 110\rangle\{1\bar{1}0\}$ dislocations as the high temperature deformation along the $\langle 001\rangle$ axis. From this we conclude that these dislocations must exist in two different core configurations.

DOI: 10.1103/PhysRevLett.87.085505 PACS numbers: 62.20.Mk, 61.72.–y, 62.20.Fe

Most ceramic materials and many intermetallic alloys are known to be brittle at room temperature. With increasing temperature these nominally brittle materials undergo a brittle-to-ductile transition (BDT) into a regime where they deform plastically due to the motion of dislocations [1,2]. The temperature at which the BDT occurs is strongly dependent on test conditions, specimen preparation, and loading rate. For example, precracked silicon under tensile loading exhibits a BDT at temperatures far in excess of 1000 K [1], while crack-free material under hydrostatic confining pressure can be deformed at 600 K [3]. Similarly, plastic deformation of brittle materials at low temperatures (LTs) can be achieved by indentation testing while the same material responds by perfectly brittle fracture under more general loading conditions. The BDT can often be rationalized by the decrease in yield stress and the corresponding increase in dislocation mobility with increasing temperature [1,2]. A case of inverse behavior, where ductility occurs with *decreasing* temperature, is reported here for the deformation of $SrTiO_3$.

$SrTiO_3$ crystallizes in the cubic perovskite structure. Since it has no phase transition above 105.5 K [4,5], it can be grown as a single crystal, and is therefore well suited as a model material for fundamental investigations of the mechanical properties of perovskites. This family of materials is abundantly available in the lower mantle of the earth; perovskites are used as electronic materials and as substrates for high temperature (HT) superconductors. However, the plasticity of $SrTiO_3$ has so far been studied only at temperatures above 1500 K [6].

Our observations were made during compression tests on $SrTiO_3$ single crystals along the $\langle 001\rangle$ and the $\langle 011\rangle$ axes between 78 and 1811 K. Specimens, of $2.5 \times 2.5 \times 6.0$ mm^3 with carefully polished side surfaces, were manufactured from single crystal boules grown by the Verneuil technique. Some preliminary results and the experimental details are described elsewhere [7]. For the $\langle 001\rangle$ compression axis, extensive plastic deformation without hardening is found at temperatures above 1500 K, and limited but very significant plastic deformation is found below 1050 K. Plastic deformation up to strains of 7% is possible at room temperature and below. The phase transition to the tetragonal structure at 105.5 K [5] apparently has no significant influence on ductility. In the low temperature regime, a plateau of constant stress is followed by significant work hardening. The length of the plateau decreases and the work hardening increases with increasing temperature. The continuing decrease in plastic deformation eventually leads to an inverse BDT at about 1050 K. Specimens with the $\langle 011\rangle$ compression axis show similar low temperature behavior but reach only 1% plastic strain.

Figure 1 shows the temperature dependence of the critical flow stress in all our experiments. Where no plasticity was observed the fracture stress is plotted. Three different regimes can be distinguished: (*A*) Below 1050 K a regime of plastic deformation at constant flow stress is followed below room temperature by an increase of flow stress with

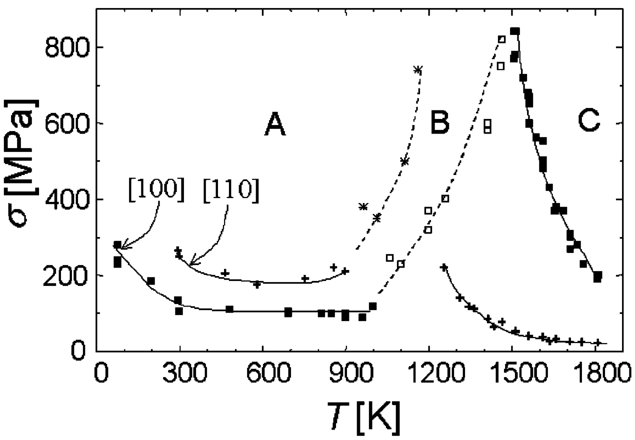

FIG. 1. The dependence of the critical flow stress σ_c on temperature T for the $\langle 001\rangle$ (filled squares) and the $\langle 110\rangle$ orientation (crosses) of the compression axis. In the intermediate temperature interval, B, where no measurable plastic deformation occurred, the fracture stress is indicated by the open squares and the stars.

decreasing temperature. (*B*) Above 1050 K the specimens shatter without plastic deformation at a stress level which increases with test temperature. (*C*) Above 1250 K the flow stress decreases drastically with increasing temperature for the $\langle 011\rangle$ compression axis; for the $\langle 001\rangle$ compression axis the same behavior is observed above 1500 K.

The macroscopic characteristics of the plastic deformation behavior are quite different in the two ductile regimes (*A* and *C*). Regime *C* is characterized by homogeneous plastic deformation, in contrast to regime *A* where deformation is inhomogeneous and concentrated in shear bands. These shear bands are directly visible in polarized light and are connected with surface steps which appear as dark lines in Fig. 2. During room temperature deformation the development of birefringence bands can be observed with the unaided eye. The orientation of the shear bands and the surface steps clearly indicates slip on $\{1\bar{1}0\}$ planes in $\langle 110\rangle$ directions in regime *A* for both specimen orientations (see Fig. 2).

Transmission electron microscopy (TEM) studies on specimens cut from the deformed crystals in an orientation parallel to the $\{1\bar{1}0\}$ glide planes predominantly reveal dislocations with a Burgers vector $b = a_0\langle 110\rangle$ (a_0 is the lattice parameter). For the $\langle 001\rangle$ compression axis, this type of dislocation dominates at all temperatures. For the $\langle 011\rangle$ compression axis it only occurs in regime *A*. Dislocations with a shorter Burgers vector, $b = a_0\langle 100\rangle$, dominate in regime *C* for this orientation. At room temperature the dislocations are more or less homogeneously distributed. At intermediate temperatures they start to cluster into dense bundles, as shown in Fig. 3. Homogeneously distributed dislocations are found again in the high temperature regime *C*.

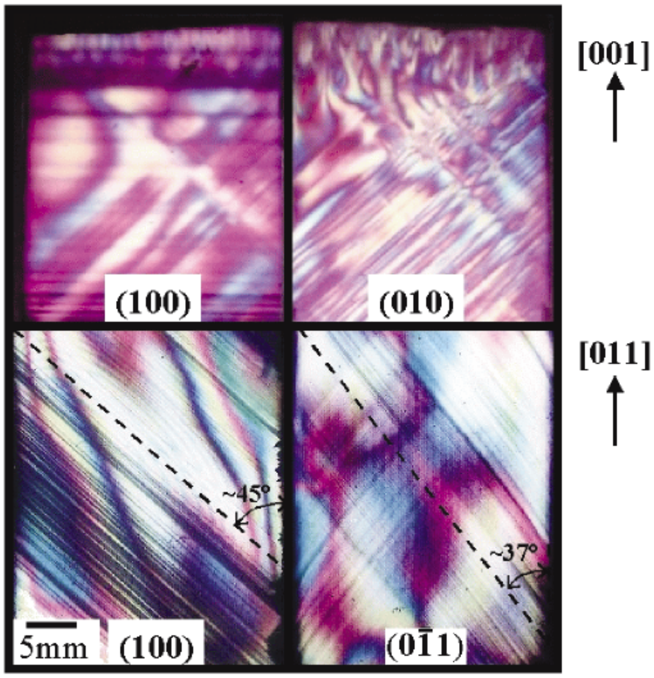

FIG. 2 (color). Images from both sides of two $SrTiO_3$ single crystals with $\langle 001\rangle$ (upper) and $\langle 011\rangle$ compression axes (lower) taken under polarized light. The crystals were deformed at room temperature to 3% and 0.6% plastic strain. Bands of birefringence are visible from both sides of the specimens. They are connected with surface steps, which appear as black lines on the images. The birefringence bands can therefore be interpreted as shear bands on which intense plastic deformation occurred. Their crystallographic orientation is parallel to $\{011\}$ planes gliding along $\langle 0\bar{1}1\rangle$ directions for both specimen orientations.

Our results in regime *C* are consistent with previous reports of high temperature deformation in $SrTiO_3$ [6]. The occurrence of two different Burgers vectors for the two different orientations of the compression axis can easily be explained, because the energetically most favorable $a_0\langle 100\rangle$ Burgers vector cannot contribute to the compressive deformation along the $\langle 001\rangle$ axis. The high temperature deformation reflects the "normal" thermally activated glide processes in ceramics [8], which most likely corresponds to the thermally activated formation of kink pairs in the dislocation line, with the subsequent motion of the kinks along the dislocation line. The high yield stresses suggest an extremely high Peierls barrier for dislocation motion, which is not unusual in ceramics [8]. A normal BDT marks the lower bound of regime *C*.

Deformation in regime *A* appears to be carried only by $a_0\langle 110\rangle$ dislocations gliding on $\{1\bar{1}0\}$ planes. The flow stress in both specimen orientations can be reconciled with a single critical resolved shear stress of $\tau_c = 50-80$ MPa at room temperature.

The fact that, for the $\langle 001\rangle$ compression axis, dislocations with identical Burgers vectors produce entirely different behavior in regimes *A* and *C* suggests that they exist with different core structures: a high temperature core which is difficult to move and a low temperature core

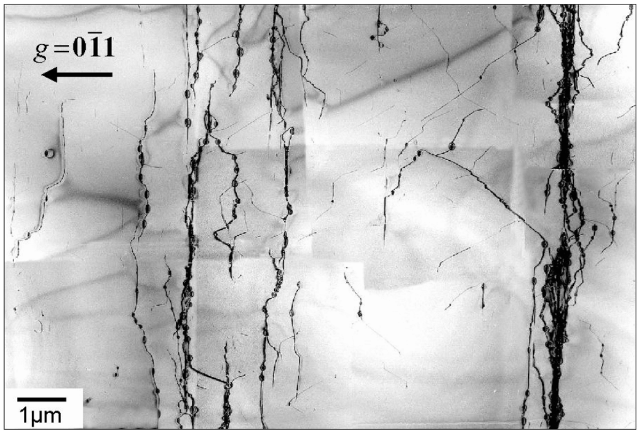

FIG. 3. Bright field TEM micrograph of the dislocation configuration after plastic deformation along the $\langle 001\rangle$ compression axis to 1% plastic strain at 815 K shows clustering of dislocations into dense bundles. The observation direction is perpendicular to the glide plane. The black spots along the dislocation line are due to the argon-ion bombardment during TEM specimen preparation.

which is much easier to move. Plasticity in regime *C* corresponds to the thermally activated glide of the HT dislocations. The much less pronounced temperature dependence of the flow stress below room temperature (Fig. 1) can be interpreted as the thermally activated dislocation glide of the LT dislocations. A similar line of thought was taken recently by Koizumi *et al.* who inferred the existence of different core structures at high and low temperatures in silicon [9], and in attempts to explain the low temperature deformation behavior of some sphalerite crystals [10,11].

The decrease of plasticity at higher temperatures, which leads to the inverse BDT at 1050 K, qualitatively resembles the flow stress anomaly of intermetallic alloys with the $L1_2$ structure [12], which consists of an increase in yield strength with increasing temperature. This anomaly can be modeled with a thermally activated locking of glissile dislocation segments [13]. Following this model, the observed deformation behavior can be rationalized with the hypothesis that the LT-dislocation structure in $SrTiO_3$ has a higher core energy than the HT-type, and can transform into the HT-type by a thermally activated process. With this hypothesis, the decrease of plastic deformation with increasing temperature can be attributed to the decreasing number (and length) of mobile LT-dislocation segments due to their transformation into HT segments, schematically depicted in Fig. 4. Since the HT segments are essentially immobile in regimes *A* and *B*, this corresponds to increased locking and a gradual loss of dislocation mobility. Possible core transformations which could lead to this behavior include the climb dissociation of the $a_0\langle 110\rangle$ dislocation in two $a_0\langle 100\rangle$ dislocations, as found, for example, in NiAl [14,15], or the change of the glide plane between the $\{110\}$ oxygen plane and the cation plane. Both of these transformations can be associated with a very significant change in dislocation core energy [16].

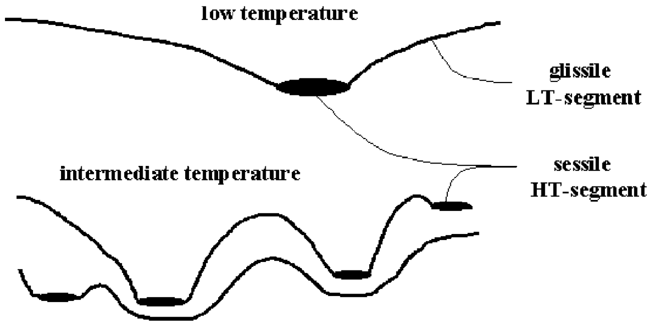

FIG. 4. Schematic drawing of partially transformed dislocation configurations. At low temperatures, only a small part of the dislocation is transformed. The transformed part can easily be surpassed by the long mobile segments and the flow stress is not limited by the transformed segments. Close to the inverse BDT temperature and in regime *B* the transformed segments are closer together and the flow stress depends on the spacing between them. Furthermore, the transformed segments act as obstacles to further dislocation motion and may even nucleate cracks.

Deformation behavior similar to $SrTiO_3$ with a transition from ductile-to-brittle and back to ductile behavior has also been reported for olivine [17] and GaAs under confining hydrostatic pressure [18]. In olivine, the origin of the brittle regime was attributed to a phase transformation which leads to the formation of so-called anticracks [17]. The brittle fracture regime *B* in $SrTiO_3$ finds a simple explanation in our core transformation model. Following this idea it is important to recall that brittle cracks can propagate at all temperatures below regime *C*. Ductility in regime *A* is observed (only) under compressive loading and because the initial crystal is free of cracks. Under these conditions, cracks must first be nucleated before they can propagate. This apparently requires some stress concentration, which could, for example, come from a pileup of dislocations at an obstacle. With the observed clustering of dislocations at intermediate temperatures (Fig. 3) it is natural to assume that a pileup of glissile LT dislocations behind a transformed sessile HT segment may be responsible for the crack initiation (indicated in Fig. 4). The increase of fracture stress with temperature can then be attributed to the increasingly higher stress required to bow out the remaining shorter segments of LT dislocation between the transformed HT segments.

The deformation and fracture characteristics of $SrTiO_3$ reported here are intimately linked to the core structure of the dislocations. Although the details of the change in core structure remain to be clarified, they are probably specifically related to the crystal structure of the material and could therefore be transferred to other materials crystallizing in the perovskite structure.

The observed low temperature ductility of $SrTiO_3$ might even allow some low temperature forming which could open ways to new applications of perovskite materials.

Finally, the documented examples of low temperature deformation in $SrTiO_3$, presented here, and in GaAs [18] strongly suggest that the role of dislocations in the plasticity of ceramics should be reconsidered and other ceramic materials should be investigated for similar behavior.

[1] S. G. Roberts, A. S. Booth, and P. B. Hirsch, Mater. Sci. Eng. **A176**, 91 (1994).
[2] P. Gumbsch, J. Riedle, A. Hartmaier, and H. F. Fischmeister, Science **282**, 1293 (1998).
[3] J. Castaign, P. Veyssière, L. P. Kubin, and J. Rabier, Philos. Mag. A **44**, 1407 (1981).
[4] F. W. Lytle, J. Appl. Phys. **35**, 2212 (1964).
[5] E. K. H. Salje, M. C. Gallardo, J. Jiménez, F. J. Romero, and J. del Cerro, J. Phys. Condens. Matter **10**, 5535 (1998).
[6] H. Koizumi, S. Katakura, T. Suzuki, T. Yamamoto, and T. Sakuma, in *Strength of Materials (ICSMA-10),* edited by H. Oikawa *et al.* (The Japan Institute of Metals, 1994), p. 737.
[7] D. Brunner, S. Taeri-Baghbadrani, W. Sigle, and M. Rühle, J. Am. Ceram. Soc. **84**, 1161 (2001).

[8] T. E. Mitchell, P. Peralta, and J. P. Hirth, Acta Mater. **47**, 3687 (1999).

[9] H. Koizumi, Y. Kamimura, and T. Suzuki, Philos. Mag. A **80**, 609 (2000).

[10] T. Suzuki, T. Nishisako, T. Taru, and T. Yasutomi, Philos. Mag. Lett. **77**, 173 (1998).

[11] T. Suzuki, T. Yasutomi, T. Tokuoka, and I. Yonenaga, Philos. Mag. A **79**, 2637 (1999).

[12] D. P. Pope, in *Physical Metallurgy,* edited by R. W. Cahn and P. Haasen (Elsevier, Amsterdam, 1996), p. 2075.

[13] D. C. Chrzan and M. S. Daw, Phys. Rev. B **55**, 798 (1997).

[14] M. J. Mills, R. Srinivasan, and M. S. Daw, Philos. Mag. A **77**, 801 (1998).

[15] R. Schroll, V. Vitek, and P. Gumbsch, Acta Mater. **46**, 903 (1998).

[16] R. Schroll, M. W. Finnis, and P. Gumbsch, Acta Mater. **46**, 919 (1998).

[17] H. W. Green and P. C. Burnley, Nature (London) **341**, 733 (1989).

[18] T. Suzuki, T. Tokuoka, I. Yonenaga, and H. O. K. Kirchner, Scr. Mater. **43**, 645 (2000).